Excluded Volume Effects in Photoinduced Electron Transfer and Geminate Recombination: Analytical Theory and Simulations

S. F. Swallen, Kristin Weidemaier, and M. D. Fayer*

Department of Chemistry, Stanford University, Stanford, California 94305

Received: August 26, 1994; In Final Form: November 16, 1994[⊗]

Analytical theory and Monte Carlo (MC) simulations are used to examine the problem of photoinduced electron transfer and geminate recombination in both infinite three-dimensional systems and in restricted geometry systems. As an example of a restricted geometry system, donor and acceptor molecules on the surface of a spherical micelle are considered. The analytical theory is an exact treatment for fixed donors and acceptors when the distance dependence of the transfer rate falls off exponentially and donor−acceptor excluded volume (DA EV) is included. Comparisons to the MC simulations, which include DA EV, show perfect agreement for both the 3D system and the micelle system. However, comparisons of the analytical theory to the simulations show that for sufficiently high acceptor concentration, acceptor−acceptor excluded volume (AA EV) becomes important. With AA EV, the analytical theory is no longer exact. A new approximate method for the inclusion of AA EV in the analytical theory is described. Comparisons with the simulations show that it is accurate up to substantial concentrations, but at sufficiently high acceptor concentrations, significant deviation from the MC simulation results are seen.

I. Introduction

A great deal of effort has been directed toward the study of photoinduced electron transfer and geminate recombination among donor and acceptor molecules in condensed matter systems. The problem can be roughly divided into two aspects, quantum mechanics and statistical mechanics. The quantum mechanical studies focus on understanding the pairwise interaction and driving force that determine the transfer rate between a donor and an acceptor at a fixed distance.[1−5] Statistical mechanics studies address the time-dependent phenomena in systems in which a donor is surrounded by a set of acceptors spatially arrayed in some configuration. The problem is to determine how the spatial distribution of acceptors determines the dynamics of forward electron transfer (donor to acceptor) and geminate recombination (the electron returns from the acceptor to the donor to recreate the initial species). It has been found experimentally and theoretically in many systems that the transfer rate can be modeled as having an exponentially decaying distance dependence.[6−9] The most straightforward spatial distribution is a donor surrounded by acceptors randomly distributed in an infinite three-dimensional system. However, the spatial distribution of donors and acceptors can have a profound effect on electron-transfer dynamics, and other geometries, such as donors and acceptors on the surface of a micelle, attached to polymer chains or in zeolites, are important.[10−13] These types of systems are referred to as restricted geometries. They are systems that are not infinite in extent and do not involve an infinite number of molecules.

Almost 30 years ago, the forward-transfer problem for a system of fixed-point particles randomly distributed in an infinite three-dimensional system was solved exactly when the transfer rate falls off exponentially with distance.[14] The result describes the time-dependent probability of finding the initially excited donor still excited at a later time $\langle P_{ex}(t)\rangle$. The decay of the probability is due to electron transfer into a randomly distributed ensemble of acceptors. The calculation is exact for the specified model.

Several years ago, the more complex problem including both forward transfer and geminate recombination (back transfer) was also solved exactly for the same model;[15−17] i.e., fixed point particles randomly distributed in an infinite three-dimensional system. This theory calculates the time dependent build up and decay of the ion pair population $\langle P_{ct}(t)\rangle$ as well as the decay of the initially excited neutral donor populations. (In $\langle P_{ct}(t)\rangle$, ct stands for charge transfer.) The initial donor and acceptor molecules are considered neutral, and electron transfer forms a cation and an anion. Back transfer regenerates the ground-state neutrals. However, the theory is general, and the initial donor and acceptor molecules can have any charge. For simplicity but without loss of generality, we will use ions to refer to the state of the system after electron transfer and neutrals to refer to the system before transfer or following geminate recombination. Recently, the exact treatment of photoinduced forward electron transfer with geminate recombination has been extended to treat restricted geometries.[18] The method is general, and as an example, the dynamics of electron transfer and geminate recombination on the surface of a spherical micelle were calculated. In this system the volume and the number of particles are finite. For the model of point particles with exponential distance dependencies for the forward- and back-transfer rates, the ensemble averages can be performed exactly in a manner analogous to the exact treatment in infinite three-dimensional systems.

The exact methods mentioned above, like those in many other electron-transfer calculations,[14,18,19] begin by assuming that the donor and acceptors are point particles. Real molecules, however, have finite sizes, and therefore it is important to assess the role of excluded volume (EV) on the dynamics of electron transfer in infinite three-dimensional systems and in restricted geometries. Excluded volume limits the distance of closest approach of an acceptor to the donor (DA EV), and it eliminates from the spatial distribution configurations in which acceptors physically overlap (AA EV).

DA EV is important at all concentrations of acceptors, and it is exactly included in the analytical theories (as in references 14−17,19) by performing the ensemble average over acceptor

[⊗] Abstract published in *Advance ACS Abstracts*, January 15, 1995.

0022-3654/95/2099-1856$09.00/0

configurations with a short distance cutoff. However, AA EV cannot be included exactly. The exact analytical method depends on the separability of the many-body problem into the superposition of two-body problems. This is possible for forward transfer and geminate recombination for point particles with DA EV.[14-17,19,20] Including AA EV requires a many particle correlation function, and therefore the problem is no longer separable. To overcome this difficulty, we have developed an approximate method that takes AA EV into account through a pair correlation function.

The continuum limit of the Blumen lattice model[21-23] has previously been used to include AA EV.[16,24,25] In the limit of low concentration, when particle interaction represents only a small perturbation on the point particle system, this method should work well. Fundamental questions arise about AA EV. How important is it? Up to what concentrations can it be ignored and the exact point particle results with inclusion of DA EV be employed? How well does the lattice model taken in the continuum limit work, and up to what concentration? Can AA EV be modeled with our new approximation based on the pair correlation function appropriate for the specific system, and if so, up to what concentration? To understand the concentration dependence of forward electron transfer and geminate recombination, these questions need to be answered.

To address these questions, the results of calculations with the analytical theories are compared to Monte Carlo (MC) simulations. It is possible to include both DA EV and AA EV in the MC simulations. Significant care was given to ensure convergence and accuracy of the simulations. DA EV is included in all of the analytical calculations, since it can be handled exactly. Comparison of the simulations and the analytical theory for three dimensions with only DA EV confirms that the analytical theory ensemble averages are performed correctly. When AA EV is included in the simulations but not in the analytical theory, it is possible to determine the range of concentrations over which AA EV can be neglected. At higher concentrations, AA EV is important and significant deviations are seen between the simulations that include it and the analytical theory which does not. It is also found that the lattice method for taking AA EV into account in the analytical theory does not do a satisfactory job.

A second approach is presented as a means of accounting for AA excluded volume in the analytical theory. The spatial distribution of finite-volume particles is taken to be a separable probability function, and thus an a priori description of particle positions can be utilized. This method is referred to as the separable probability distribution (SPD). In infinite three dimensions, a radial pair-separation distribution function, obtained from numerical solutions to the Percus-Yevick (PY) approximation for hard spheres, is employed. This weighted distribution is utilized to account for the effects of AA excluded volume on the state probability functions, $\langle P_{ex}(t)\rangle$ and $\langle P_{ct}(t)\rangle$. Comparison of this approach is made to MC simulations for several acceptor concentrations and several sets of electron-transfer parameters.

The AA EV problem in restricted geometries is also examined by performing the same types of studies for the micelle problem. Simulations with DA EV are compared to the exact analytical theory with DA EV to demonstrate the accuracy of the ensemble average. Simulations with DA EV and AA EV are compared to the analytical results obtained with only DA EV to determine the range of concentrations (fractional surface occupancy) in which AA EV is not important. Then the SPD method for the micelle problem is employed to determine its utility for restricted geometry systems. Also, comparisons between the solutions of the three-dimensional (3D) problem and the micelle problem is used to illustrate the effects of restricted geometry on electron-transfer dynamics.

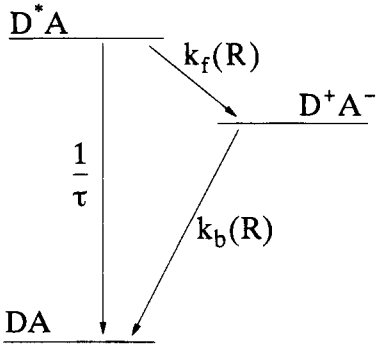

Figure 1. Three-level system composed of the ground-state neutrals (DA), electronically excited-state neutrals (D*A), and ionic pair (D^+A^-). k_f and k_b are the rate constants for forward and backward (geminate) electron transfer, respectively, and τ is the excited-state lifetime.

The results for both the 3D and the micelle dynamics demonstrate that there is a significant range of concentrations in which AA EV can be neglected. However, at moderate concentration, the errors are significant. For both forward- and backward-transfer probability calculations, the SPD method does a better job of improving the accuracy in the moderate concentration range than does the continuum limit of the lattice method (hereafter referred to as CL). The SPD works better for the calculation of $\langle P_{ct}(t)\rangle$ than of $\langle P_{ex}(t)\rangle$. In limiting cases when the rates of electron transfer become quite rapid, such as high acceptor concentration, or the use of very long range-transfer parameters, even the SPD method fails. In these cases, only the simulation can provide accurate results. At intermediate concentrations, the analytical theories are important because the vast amount of computational time required to perform the simulations may make them unusable for data analysis.

II. Methods for MC Simulations and Analytical Theory

The model under consideration is a three-level system, composed of a neutral ground state (DA), an electronically excited state (D*A), and an ion pair formed by forward electron transfer (D^+A^-). This is illustrated in Figure 1. The forward- and backward-transfer rate constants are given by $k_f(r)$ and $k_b(r)$, respectively, and τ is the excited-state lifetime in the absence of electron transfer. The donors are considered to be present in sufficiently low concentration that each will interact only with acceptors and not with other donors. This precludes any excitation hopping to other donors by Förster energy transfer. Following photoexcitation, the donor molecule can either directly relax to the ground state or undergo forward electron transfer to one of the acceptors. If the latter occurs, the ion pair may exist for a time before geminately recombining. The master equations for such a three level system of one donor surrounded by N acceptors, each at a given distance R_i from the donor, are

$$\frac{\partial}{\partial t} P_{ex}(\bar{R},t) = -\left[\frac{1}{\tau} + \sum_{i=1}^{N} k_f(R_i)\right] P_{ex}(\bar{R},t) \qquad (1)$$

where $P_{ex}(\bar{R},t)$ is the time-dependent probability that a donor molecule, excited at time $t = 0$, is still in the excited electronic state at a later time t. $\bar{R}$ is used to designate the particular configuration of the acceptor particle positions (R_1, ..., R_N), with the donor at the origin. The rate constant $k_f(R_i)$ characterizes forward electron transfer from the excited donor to the ith

acceptor at separation distance R_i, and

$$\frac{\partial}{\partial t}P^i_{ct}(\bar{R},t) = k_f(R_i)\,P_{ex}(\bar{R},t) - k_b(R_i)\,P^i_{ct}(\bar{R},t) \qquad (2)$$

where $P^i_{ct}(\bar{R}, t)$ is the probability that the ith acceptor exists as an anion at time t, and $k_b(R_i)$ is the rate constant for geminate recombination. The rate constants for excited-state decay and forward and backward transfer are given by

$$k = 1/\tau$$

$$k_f(R) = \frac{1}{\tau}\exp\left(\frac{R_f - R}{a_f}\right)$$

$$k_b(R) = \frac{1}{\tau}\exp\left(\frac{R_b - R}{a_b}\right) \qquad (3)$$

where τ is the excited-state lifetime. The parameters R_f and R_b define the distance scale of forward and backward transfer, respectively, and a_f and a_b parametrize the falloff of the transfer rate with distance between donor and acceptor. The set of differential equations has been solved in two manners: integration by means of Monte Carlo simulation, and an averaging procedure over all possible acceptor positions, which gives an explicit analytical form. The latter has been well documented in the literature,[15-17] but the salient results will be presented here.

A. Analytical Solutions. For the 3D system at low concentrations, the ensemble average of the excited-state probability was obtained analytically by Inokuti and Hirayama.[14] For point particles (no excluded volume), the IH result is

$$\langle P_{ex}(t)\rangle = \exp\left(-\frac{t}{\tau}\right)\exp(-4\pi C\int_0^\infty [1 - \exp(-k_f(R)t)]R^2\,dR) \qquad (4)$$

where C is the acceptor concentration. The solution to eq 2, giving an analytical expression for the time-dependent ion-state probability, requires numerical averaging over all $(N - 1)$ acceptors which did *not* receive the electron. By first averaging eqs 1 and 2 over these indistinguishable, randomly distributed neutral particles, an expression can be found for $\langle P_{ct}(R,t)\rangle_{N-1}$. When this is averaged over the last spatial position R and then summed over all N acceptors and taken to the thermodynamic limit (as the number of particles N and the system volume V each go to infinity, the ratio of N/V goes to the concentration C), the solution for point particles is[16,26]

$$\langle P_{ct}(t)\rangle = 4\pi C\int_0^\infty\int_0^t k_f(R)\exp(-k_f(R)t')\langle P_{ex}(t')\rangle \times \exp(-k_b(R)(t - t'))dt'\,R^2\,dR \qquad (5)$$

Equations 4 and 5 give *exact* solutions to the probability-state functions. The initial photoexcitation is taken to occur at time $t = 0$, thus $\langle P_{ex}(t=0)\rangle = 1$, and $\langle P_{ct}(t=0)\rangle = 0$. These formulas are straightforward to calculate numerically. In practice, a maximum value is set for the upper radial limit of integration such that all relevant transfer events are included in the calculations. This limit is made large enough that further increase in radial integration yields no change in the observed curves.

Similarly, the master equations can be solved exactly for any restricted geometry. However, for many restricted geometry problems, such as the micelle problem discussed here as an example, there are a finite number of acceptors. Therefore, the averages do not pass to the thermodynamic limit. Unlike the Inokuti and Hirayama result for the infinite 3D problem, there is an explicit dependence on the number of acceptors. The solutions for the point particle state probability functions for molecules on the surface of a spherical micelle are

$$\langle P_{ex}(t)\rangle = \exp\left(-\frac{t}{\tau}\right)\left[\frac{1}{2R_{mic}{}^2}\int_0^{2R_{mic}}\exp(-k_f(R)t)R\,dR\right]^N \qquad (6)$$

$$\langle P_{ct}(t)\rangle = N\int_0^{2R_{mic}}\int_0^t k_f(R)\exp\left(-\frac{t'}{\tau}\right)\exp(-k_f(R)t')\exp(-k_b(R)(t - t'))\left[\int_0^{2R_{mic}}\exp\left(-\frac{t'}{\tau}\exp\left(\frac{R_f - R'}{a_f}\right)\right)\frac{R'}{2R_{mic}{}^2}\,dR'\right]^{N-1} \times dt'\,\frac{R}{2R_{mic}}\,dR \qquad (7)$$

Here R_{mic} is the micelle radius, which gives an absolute upper limit on the system size and separation distance between donor and acceptor. The results presented in eqs 6 and 7 are discussed in detail elsewhere.[18]

B. Simulations. To examine the importance of excluded volume (discussed below) and to verify the exact analytical theory used to obtain the solutions given in eqs 4–7, the differential equations (1) and (2) were directly solved and then averaged by means of Monte Carlo (MC) simulation. The expressions for the state probability functions are identical for both the infinite 3D system and the micelle surface system. The differences between the two problems is the spatial distribution of acceptor positions. Because of the strong distance dependence of electron transfer, the geometrical restrictions imposed by a spherical surface strongly affect the results of the calculations.

The most critical and time-consuming requirement when performing the MC simulations is to obtain an appropriate initial placement of acceptors. For the case of noninteracting point particles this is straightforward; the donor and each acceptor can be placed independently according to the geometrical restrictions of the system. The spatial distributions are random. For one random spatial arrangement $\bar{R}$ of all N acceptors at time t, the solution to eq 1 for both the infinite 3D and the micelle system is

$$P_{ex}(\bar{R},t) = \exp\left(-\frac{t}{\tau}\right)\exp(-\sum_{i=1}^N k_f(R_i)t) \qquad (8)$$

It is readily shown that the solution to eq 2 for an arbitrary configuration of N acceptors is given by

$$P_{ct}(\bar{R},t) = \sum_{i=1}^N \frac{k_f(R_i)}{k_b(R_i) - \frac{1}{\tau} - \sum_{j=1}^N k_f(R_j)}\left[\exp\left(-\frac{t}{\tau} - \sum_{j=1}^N k_f(R_j)t\right) - \exp(-k_b(R_i)t)\right] \qquad (9)$$

To obtain the ensemble-averaged values of these functions, the average over many different acceptor configurations is performed. Enough trials must be included to sufficiently span the configuration space, giving a complete and random selection

of acceptor placements. In practice these simulations are straightforward to perform, although they are time consuming.

All the Monte Carlo simulations employed a random number generator (rng) to uniformly select values in the range 0−1. These values were then used to sample the ranges of the functions of interest. The algorithm to select random numbers was developed by Marsaglia and Zaman[27] and was chosen because of its extremely large period ($\sim 10^8$) and its ability to satisfy recognized statistical tests. This algorithm required 24 input seed numbers, which were obtained from a simpler rng with a shorter period.[28]

For the 3D isotropic point particle model, the donor was placed at the origin of a spherical volume. Each acceptor was placed by randomly choosing a value for all three of the spherical coordinate quantities r, ϕ, and θ. For each coordinate, a random number F was chosen in the set (0−1). The radial coordinate is independent of ϕ and θ and thus can be freely chosen on a randomly sampled weighted distribution. The probability of an acceptor being placed at the distance r is given by

$$P(r) = \frac{4\pi r^2}{(^4/_3\pi R_v^3)} \tag{10}$$

where R_v is the maximum radial distance of the system being considered. Thus the mapping of the uniform distribution F into the weighted distribution for R is obtained from the incomplete integral of $P(r)$ determined by the upper limit R':

$$F = \int_0^{R'} P(r)\,dr = \int_0^{R'} \frac{4\pi r^2}{4/3\pi R_v^3}\,dr \tag{11}$$

The inversion of eq 11 then gives the choice of R':

$$R' = R_v\sqrt[3]{F} \tag{12}$$

The azimuthal angle ϕ is chosen independently from $[0-2\pi]$. It is uniformly distributed in this range, and thus $\phi' = 2\pi F$. The third degree of freedom, the polar angle θ, can have values in the closed set $[0-\pi]$. Statistically, however, the choice of θ must be weighted by the relative point density on a spherical surface as a function of polar angle. A uniform distribution in the range of θ would result in an incorrectly high point density near the spherical poles. Instead, the normalized distribution is given by $P(\theta) = 1/2 \sin\theta$. Again performing an incomplete integral, this time for the polar angle from 0 to θ', gives a value $\theta' = \arccos(1 - 2F)$.[29]

For each configuration of acceptors about one donor, all particles were placed according to the randomly chosen vector components $[r_i, \phi_i, \theta_i]$. The number of particles N was determined by the choice of acceptor concentration and the system volume. The calculated observables were then determined by summing over all acceptors. This process was repeated many times, until a convergence in the physical observables had been obtained. As with the analytical routines, the spherical radius was increased past the point at which any change was observed. The number of configurations required to reach convergence was, in large part, dependent upon the concentration of particles in the system. As the molarity was increased, the rate at which the configuration space was sampled increased concomitantly. For point particle concentrations of up to 0.3 M, typically 10^5-10^6 configurations were averaged. This was repeated for varying concentrations and different electron-transfer parameters.

By restricting particles to lie on a spherical surface, the micelle system was limited to a particular size and thus was not averaged in the thermodynamic limit. Therefore, the state probability functions were calculated for specific numbers of acceptor particles N. Particles were placed by choosing angular variables ϕ_i and θ_i, each with a given radial component R_{mic}, defined as the micelle radius. A total of $N + 1$ particles were placed, and one of them randomly chosen to be the donor molecule. Chord separation distances between the donor and all other N particles were found, and the physical observables calculated. As in three dimensions, the ensemble average was obtained by creating and averaging over many such configurations.

III. Excluded Volume

To account for the physical size of real molecules, excluded volume must be included in the models. For the isotropic 3D case, all particles were assumed to be spherical in shape, and a hard-sphere model was used to approximate particle interaction and excluded volume. For the micelle, particles were taken to be curved hard disks (hard disks with the same radius of curvature as the micelle),[30] resting on the micelle surface.

A. Donor−Acceptor Excluded Volume. The most significant form of volume exclusion is between donor and acceptor. This is because the area in which electron transfer happens most readily, the region closest to the donor, is inaccessible. As a result, the average rates of both forward and back transfer are dramatically lessened. For the analytical theory, only two changes need to be made to eqs 4−7. First, the lower limit of integration over space must be changed from zero to the value of the donor−acceptor contact distance: the sum of the donor and acceptor radii. Second, the volume term, which is present in the concentration C, must be decreased appropriately to account for the decreased volume over which the final R integral is being performed. For the isotropic case, the volume term changes from $V = {}^4/_3\pi R_v^3$, where R_v is the maximum limit of integration and now becomes ${}^4/_3\pi(R_v^3 - R_m^3)$, where R_m is the contact distance for donor and acceptor. Similarly, the area term for the micelle problem is normalized over the resulting restricted surface volume.[18]

Inclusion of DA excluded volume in the MC simulations introduces a more complex issue concerning the randomness of initial particle placement. It is important to include in the statistical analysis only those configurations which have no overlap between any particles. This can be accomplished by one of two methods. The first is to place all N particles randomly in space, regardless of where any other particles may be, and subsequently reject all configurations which result in any DA overlap. New configurations then need to be created until an acceptable one has been found. A second means is to force all the acceptors to be placed only in allowed positions (i.e., outside the donor volume) and then equilibrating all positions to achieve a random configuration. The latter method of position equilibration is in general much more efficient for creating an initial set of particle placements. Experimentally, this is accomplished by randomly placing each acceptor anywhere in the system volume. If any particle is found to overlap the donor, it is replaced in a new position. After creating an entire configuration of N particles, all acceptors are then moved randomly, with the limitation that no movements resulting in overlap are accepted. This is continued until the particle correlation due to the initial placement requirements is destroyed. In this manner, diffusive motion is simulated, and an effectively random initial condition is established. The methods used to equilibrate particles will be more fully described

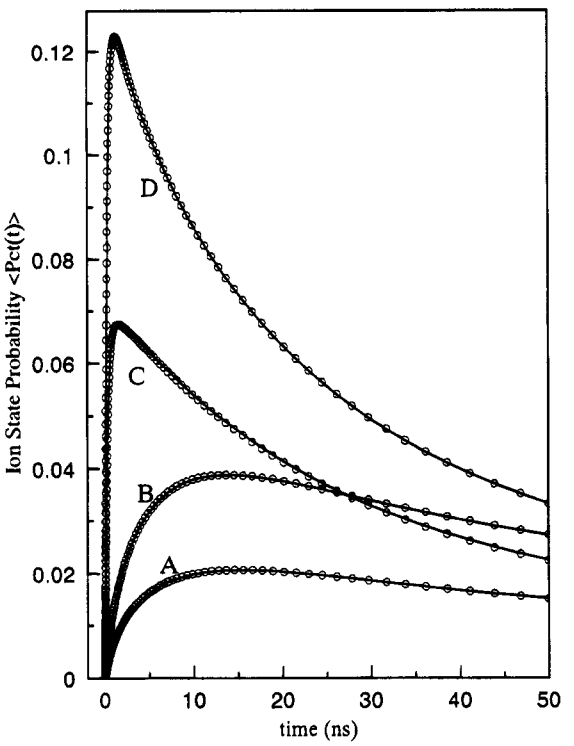

Figure 2. Ion pair survival probability $\langle P_{ct}(t)\rangle$, calculated by both analytical theory (solid lines) and MC simulations (circles) for 3D isotropic system. Donor–acceptor contact distance of 10.0 Å. Acceptor concentration for curves A and C is 0.166 M, and for B and D is 0.332 M. Fluorescence lifetime $\tau = 15.0$ ns. Electron-transfer parameters for curves A and B: $a_f = 1.0$, $R_f = 10.0$, $a_b = 1.0$, $R_b = 10.0$; for curves C and D: $a_f = 0.5$, $R_f = 12.0$, $a_b = 1.0$, $R_b = 10.0$.

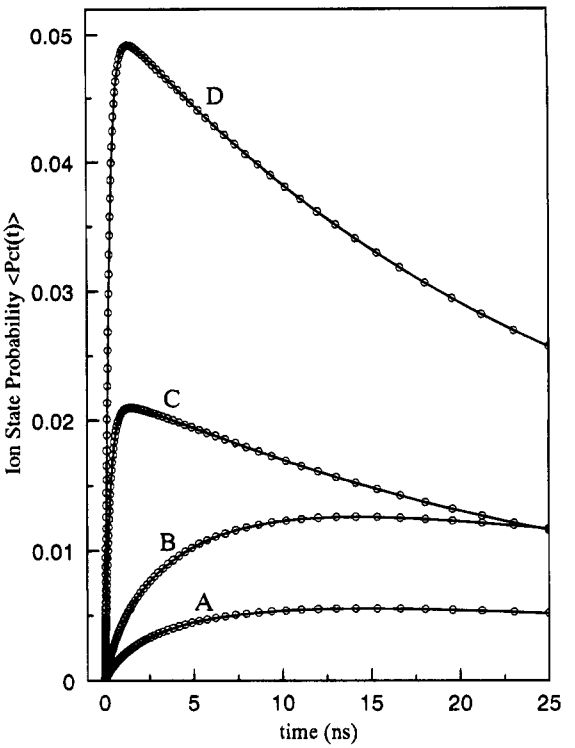

Figure 3. Ion pair survival probability $\langle P_{ct}(t)\rangle$ for micelle surface, calculated by both analytical theory (solid lines) and MC simulations (circles). Donor–acceptor contact distance of 10.0 Å. Micelle radius $R_{mic} = 24.6$ Å. Curves A and C have five acceptor particles, and curves B and D have 10 particles. Fluorescence lifetime $\tau = 15.0$ ns. Electron-transfer parameters for curves A and B: $a_f = 1.0$, $R_f = 10.0$, $a_b = 1.0$, $R_b = 10.0$; for curves C and D: $a_f = 0.5$, $R_f = 12.0$, $a_b = 1.0$, $R_b = 10.0$.

below. For point particle acceptors, the number of equilibration steps required to destroy any initial correlation is small. Typically the number of steps was 4 or 5 times N.

The numerical calculations were done on an IBM RS6000 Model 375 workstation. All programs were written in the C language. Several standard subroutines were obtained from algorithms written by Press et. al.[31] The analytical calculations for both the 3D and micelle systems required less than 20 s of CPU time. The Monte Carlo simulations required upward of 12 h to complete.

While the analytical solutions for the 3D system with donor–acceptor excluded volume (DA EV) but no acceptor-acceptor excluded volume (AA EV) have been shown to be mathematically exact, the validity of the numerical averaging techniques can be further demonstrated by comparison with the Monte Carlo simulations. In Figure 2, $\langle P_{ct}(t)\rangle$ curves for the infinite three dimensions DA EV problem are given for two different acceptor concentrations, each calculated for two sets of electron-transfer parameters. (The parameters are given in the figure caption.) Each curve is actually a superposition of two methods of computation: analytical theory from eq 5 (solid lines) and the Monte Carlo simulation from an ensemble average of eq 9 (circles). It is clear that the agreement between the analytical theory and the simulations is perfect for all concentrations and electron-transfer parameters at all times. A wide range of concentrations, particle sizes, and transfer parameters were examined for both forward and backward electron transfer, with every case showing exact agreement between the simulations with DA EV and the analytical theory with DA EV. Thus, it can be emphasized that the analytical theory is an *exact* expression for the state probability functions.

DA excluded volume has a significant impact on the dynamics of electron transfer with geminate recombination. The ensemble averaged time dependence of both forward and back transfer are slowed by the spatial limitation. For all sets of transfer parameters, the probability maxima is shifted to later times when DA EV is included. Also, the magnitude of the maximum ion probability is increased. Although the forward transfer happens more slowly in this case, thus creating fewer total ions in a given time span, the slowed back transfer allows each ion pair to survive for a longer time. This effect varies with particle size and excited-state lifetime but is seen as a general trend.

Similar agreement between simulations with DA EV and analytical theory with DA EV is shown for the micelle calculations. Figure 3 shows the DA EV results for this restricted geometry. (See figure caption for parameters). Both methods of computation are shown, and the agreement is perfect at all times.

The comparisons of the analytical and simulation calculations presented above (which include DA EV but do not include AA EV) confirm that the analytical theory is exact, the numerical procedures are correct, and that the simulation procedures are correct. This is true for both infinite 3D systems and restricted geometry systems. The method is general and will work for systems of any dimensionality and for any restricted geometry. However, the sphere surface problem is a special case of the general problem because the ensemble average is translationally invariant; i.e., the ensemble average about a donor located at any position on a sphere is the same. Therefore, it is not necessary to perform an additional average over starting points. For systems such as polymers, this will not be the case. This has been treated extensively for the problem of electronic excitation transfer in restricted geometries.[23,32,33] For a system in which the ensemble average is not translationally invariant, first the ensemble average is performed over all configurations

about a starting point, and then an additional average is performed over starting points. It is not sufficient to perform the average for some average starting point. The additional average over starting points will make the calculation more time consuming, but it does not fundamentally change the nature of the method presented above.[29,34]

B. Acceptor−Acceptor Excluded Volume. In addition to donor−acceptor overlap, particle placement is also significantly affected by acceptor−acceptor excluded volume. This further complicates the problem of the spatial distribution of particles and influences the dynamics of electron transfer at sufficiently high concentrations. Unlike DA EV, which is important at all acceptor concentrations, AA EV becomes increasingly important as the concentration is raised. By comparing MC simulations that include both DA EV and AA EV with the analytical theory that only contains DA EV, it is possible to determine the range of concentrations in which AA EV becomes important.

i. Blumen Lattice Method. Previous work has incorporated the continuum limit of the Blumen lattice model[21,22] (CL) into the 3D isotropic electron transfer analytical calculations.[16,24,25] The Blumen model allows particles to be placed only at lattice sites, which are separated by the two-particle contact distance. The probability of site occupancy is determined by the acceptor concentration (number density). In this way, the statistical requirements of particle placement and volume exclusion are taken into account. Comparison to simulations can test the accuracy of this method. Equation 4, the excited state probability function including DA EV and the Blumen model for AA EV for the 3D system, can be expressed in the continuum limit of the lattice model as[16,24,25]

$$\langle P_{ex}(t)\rangle = \exp\left(-\frac{t}{\tau}\right)\exp\left(\frac{4\pi}{d^3}\int_{R_m}^{\infty}\ln[1-p+p\exp(-k_f(R)t)]R^2\,dR\right) \quad (13)$$

where d is the acceptor diameter, $p = Cd^3$, and $R_m = R_D + R_A$, the sum of donor and acceptor radii. Similarly modifying eq 5 for the 3D system gives

$$\langle P_{ct}(t)\rangle = 4\pi C\int_{R_m}^{\infty}\int_0^t \frac{k_f(R)\exp(-k_f(R)t')}{1-p+p\exp(-k_f(R)t')}\langle P_{ex}(t')\rangle \exp(-k_b(R)(t-t'))\,dt'\,R^2\,dR \quad (14)$$

These expressions are written in the limit that the discrete lattice model is extended to infinite size at constant concentration, thus describing a continuum approximation to the lattice model. This approximation is useful when dealing with solvents such as liquids and disordered glasses which do not have a static, organized molecular structure. Similar expressions for the micelle problem do not exist.

ii. Separable Probability Distribution (SPD) Method. As will be shown below, the continuum lattice method (CL) does not work very well. We have developed a new approach, called the separable probability distribution (SPD) method. This method is superior to the CL method, but it also fails at sufficiently high concentrations and sufficiently rapid transfer parameters.

Equations 4−7 can be recast to implement the new method that accounts for the effects of AA EV. When all particles are taken to have zero volume, their positions are uncorrelated, and the total radial probability can be separated into a product of individual probabilities $P(\bar{R}) = p(R_1)\,p(R_2)...p(R_N)$, where $p(R_i)$ is the probability that a particle will be found at distance R_i. $p(R_i)$ is independent of all other particles, i.e., there is a separable probability distribution. Conversely, when acceptors have a nonzero volume, their positions become correlated, and the radial probability must be written $P(\bar{R}) = P(R_1,R_2,...R_N)$. Since the solvent is treated as a continuum (see discussion in section IV), as the acceptor concentration is increased, this probability is seen to have radial variations in local density caused by the excluded volume. An approximation can be made, however, that $P(\bar{R})$ is separable into N two-particle probability distributions, $P'(R)$. As a result, the correlated radial pair probability function $P'(R)$ can be written as the product of the uncorrelated function $P(R)$ and a pair-distribution function $g(R)$ which accounts for variations in local density:

$$P'(R) = g(R)\,P(R) \quad (15)$$

This is the separable probability distribution (SPD) approximation. The new function $P'(R)$ must be correctly normalized by forcing it to integrate to 1 over the available system volume. The function $g(R)$ describes the probability of finding two particles with the separation R, relative to the probability of finding this separation in a system of uniform particle distribution at the same density. Thus, when all particles have zero volume, the positions are uncorrelated and $g(R)$ is uniformly equal to 1 at all values of R. In this limit, $P'(R)$ is identical to the random 3D distribution $P(R)$. When excluded volume is considered, positions become correlated, and $g(R)$ describes the resulting radial density variations.

Examples of the pair distribution function $g(R)$ have been obtained for various models of molecular interaction, such as a Lennard-Jones potential, sticky spheres, and hard spheres.[35−37] An exact solution to the Percus−Yevick (PY) equation has been developed for a system of hard spheres.[38−40] Several algorithms have been published[38,41,42] that allow for fast numerical computation of $g(R)$ values using the PY hard-sphere formalism.

If the SPD assumption is made, the function $P'(R)$ can be used to describe the particle distribution in the analytical expressions for the physical observables. In the case of nonzero volume this distribution is not rigorous because the probabilities are not mathematically separable. However, it presents only a minor functional change to the theory and is easily implemented. The validity and usefulness of this approximation can be determined by comparison with the MC simulations. The expression for the infinite 3D isotropic excited-state probability becomes

$$\langle P_{ex}(t)\rangle = \exp\left(-\frac{t}{\tau}\right)\exp(-4\pi C\int_{R_m}^{\infty}[1-\exp(-k_f(R)t)]g(R)R^2\,dR) \quad (16)$$

where this equation is the same as eq 4, except for the inclusion of DA EV by limiting the volume integral with R_m, and by accounting for AA EV with $g(R)$.

Modifying eqs 5−7 to implement the SPD approximation for the new particle distribution $P'(R)$ for the other physical observables in both the 3D and micelle systems can be done simply by replacing the point particle $P(R)$ with the new function $P'(R)$. This approximation can be used for systems of any geometry. Appropriate values for $g(R)$ must be used which correspond to the packing fraction η, defined by the concentration C and particle diameter d. For the 3D system with spherical particles, the packing fraction is defined as $\eta = \pi\varrho d^3/6$, where ϱ is the average local density and d is the particle diameter. ϱ is calculated using a "reduced" volume: using only the volume of the system which is not excluded from acceptor placement by donor volume. For the micelle case,[18] it is defined as

$$\eta = N\left(1 - \cos\frac{r_a}{R_{mic}}\right)\Big/\left(1 - \cos\frac{r_d}{R_{mic}}\right) \quad (17)$$

where N is the number of acceptors, r_a and r_d are one-half the arc length of the acceptor and donor disks, respectively, and R_{mic} is the radius of the micelle. Values for the 3D isotropic $g(R)$ can be obtained either from numerical computation,[38,42] tabulated values in the literature,[43] or from the pair distribution determined in MC simulations, as described below. Analytic solutions for $g(R)$ in the restricted geometry of the micelle do not exist. In this case, pair distribution functions must be obtained directly from the many-particle simulations.

iii. Monte Carlo Simulations with AA Excluded Volume. Inclusion of acceptor volume in the Monte Carlo simulation requires a vast increase in computational effort. When placing each acceptor, it is necessary to check overlap between it and all other particles, including the donor. For all but the lowest concentrations, overlap was found to be extremely common, and the use of equilibration to eliminate particle placement correlation and obtain the correct hard-sphere $g(R)$ was required. Details concerning equilibration are given in the literature,[36,37,44] but a description of our methods will be presented. For the 3D system with equilibration it was necessary to use a Cartesian system with the origin at the center of a cube. Given a cube with sides of length L, each of three axis coordinates for each particle was chosen independently on $[-L/2 - +L/2]$, giving a unique position in the cube. After placing all N particles in the system (replacing any which encountered overlap), each molecule was moved independently. This was accomplished by again choosing Cartesian coordinate values for x_{eq}, y_{eq}, and z_{eq} and then adding vectorally to the initial particle placement. If this new position was found to not overlap any other particle, the step was accepted. If overlap was encountered, the motion was rejected, and the particle remained in its initial position. This was repeated many times for all N particles, until a condition of equilibration was obtained. The magnitude of the step distance r_{eq} was adjusted for each concentration, such that approximately half of all equilibration motions resulted in overlap and were rejected.[37]

For the micelle surface, equilibration was done similarly, except the vectors of motion were chosen given the corresponding geometrical requirements.[18] A coordinate transform shifted the particle in question to a temporary coordinate origin at the north pole, and an azimuthal angle ϕ_{eq} chosen randomly on $[0-2\pi]$. Given a chord length of motion r_{eq}, the particle was moved to the new location. This position was then transformed back into a coordinate system in which the origin resides at the spherical north pole.

To limit the size of the 3D isotropic model being considered and thus limit the computational time required, the minimum image convention with periodic boundary conditions was employed.[37,45] A primary cube was created using the initial conditions described above. An identical image of this cube was then mathematically repeated in every direction, creating an infinite system. Any motion of a given particle was assumed to be occurring simultaneously to all of that particle's images in every cube. Thus, if a particle moved outside the primary cube along one axis, that particle's image in the adjoining cube would move into the primary cube across the opposite face. Mathematically, if any of the three Cartesian coordinates, labeled α, for particle i became greater than $L/2$ or less than $(-L/2)$ after any equilibration move (i.e., if it moved outside the primary cube along the α axis), it was reflected back into the cube across the opposite face by the coordinate transformation:

$$\begin{aligned} &\text{if } r_{\alpha i} > L/2, && r_{\alpha i} \rightarrow r_{\alpha i} - L \\ &\text{if } r_{\alpha i} < -L/2, && r_{\alpha i} \rightarrow r_{\alpha i} + L \end{aligned} \quad (18)$$

Due to the short range of electron transfer, particle interactions were considered only between the donor and the acceptors within the primary cube. The system was made large enough that transfer events to particles with D−A separations larger than $L/2$ were insignificant. This size was dependent upon the chosen electron-transfer parameters and the concentration of acceptors but was always significantly less than the value of 40 Å used in the simulations.

The micelle calculations did not require similar periodic approximations because the system was constrained by the absolute size of the micelle. Electron transfer was considered only between particles on a single micelle surface. Further considerations, such as intermicellar transfer between particles on several different micelles in solution, were not evaluated.

The method of equilibration has the advantage of requiring only one initial particle configuration to be laid down. This set of placements is then equilibrated, typically with more than 10 000 total particle motions. Following this, particle sites are taken to be uncorrelated with their initial positions, and calculation of the physical observables is done for the configuration. All particles are then equilibrated again, and calculation of the observables is performed for this new configuration. This is repeated many times, and the resulting calculations averaged together. Particular configurations were seen to be weakly correlated with those before and after it, but sufficient equilibration was done to ensure a full sampling of configuration space.[37,44] The number of configurations required to reach convergence in the calculated functions was inversely related to concentration and was found to be on the order of 10^4 or 10^5.

iv. Pair Distribution Functions, g(R). In addition to the physical observables calculated by the MC simulations, ensemble-averaged values for the pair distribution function were obtained. Again using a minimum image convention with periodic boundary conditions for the infinite 3D system, the separation between particles i and j was determined by the closest image of j to particle i. For the separation distance between particles i and j for each Cartesian coordinate α:

$$\begin{aligned} &\text{if } r_{\alpha ij} > L/2, && r_{\alpha ij} \rightarrow r_{\alpha ij} - L \\ &\text{if } r_{\alpha ij} < -L/2, && r_{\alpha ij} \rightarrow r_{\alpha ij} + L \end{aligned} \quad (19)$$

Calculation of $g(R)$ was done by determining the distance between each pair of particles in each configuration and building a histogram of separations. The array of values was normalized by dividing by the total number of possible pairs in a configuration of N particles, $N(N-1)$, and by the number of configurations in the average. It was then divided by ϱ, the average density for a uniform distribution of uncorrelated point particles.

As mentioned above, for the infinite 3D system, the PY formalism provides an analytical method for obtaining $g(R)$. In the 3D calculations presented below, the PY $g(R)$ was used. Comparison between the PY $g(R)$ and those obtained from the simulations showed perfect agreement. However, no analytical method exists for determining the $g(R)$ for hard curved disks on the surface of a sphere. An approximate method has been developed.[18] In the calculations presented below, the $g(R)$ for the micelle problem was obtained from the simulations and then used in the analytical theory. By using the $g(R)$ obtained from the simulations, any difference between the analytical results

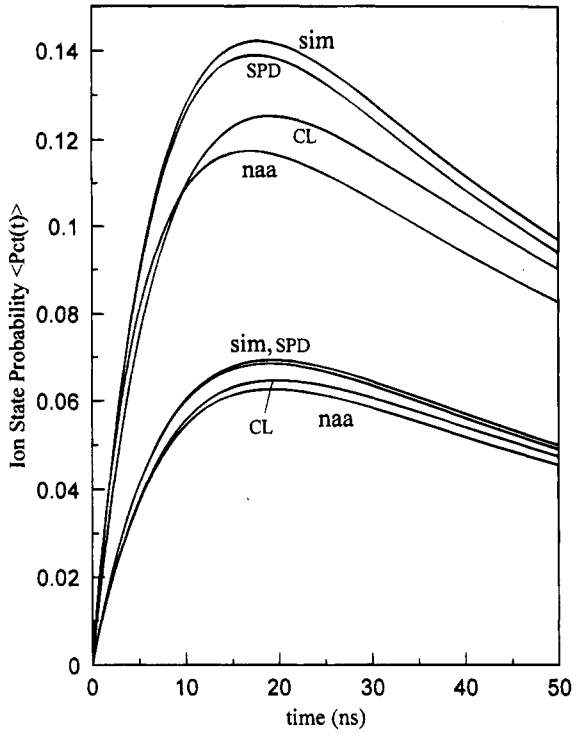

Figure 4. Ion survival probability $\langle P_{ct}(t)\rangle$ for infinite 3D system with acceptor–acceptor excluded volume, as calculated by several different methods: MC simulations (sim), separable probability distribution (spd), continuum limit of the lattice model (CL), and exact theory with no inclusion of AA EV (naa). Each method of calculation is given for acceptor concentrations of 0.166 M (lower curves) and 0.332 M (upper curves). All molecules have a radius of 5.0 Å. Fluorescence lifetime τ = 15.0 ns. Electron-transfer parameters for all curves are $a_f = a_b$ = 1.0, $R_f = R_b$ = 10.0.

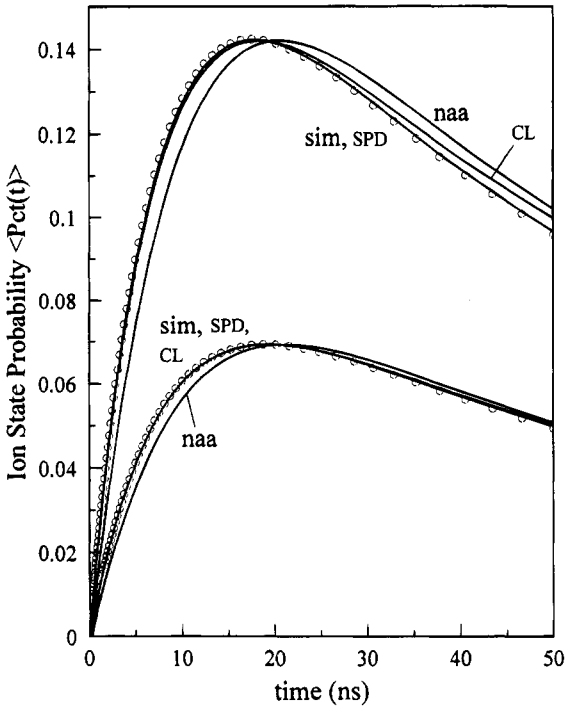

Figure 5. Ion survival probability $\langle P_{ct}(t)\rangle$ for infinite 3D system with acceptor–acceptor excluded volume calculated by several methods, all scaled in magnitude to match the MC simulations at t = 20 ns. All labels and parameters are the same as in Figure 4. The simulations are presented as open circles for comparison.

and the simulations when AA EV is included is real and not due to the use of different pair distribution functions in the two types of calculations.

v. Results of Calculations Including AA EV: Simulations and Analytical Theories. For the 3D infinite system, comparisons can be made between the four different methods of calculation (all with DA EV): analytic theories with no AA EV, using the CL method for AA EV, using the SPD method for AA EV, and MC simulations with AA EV. Figure 4 displays results for two concentrations and one set of transfer parameters (see figure caption for parameters). The ion survival probability, $\langle P_{ct}(t)\rangle$, is shown. All of the analytical methods disagree with the simulations to some extent. The disagreement becomes larger when the electron-transfer parameters give more rapid transfer rates and lead to the creation of more ions. For a wide variety of parameters and concentrations, it is always seen that the CL method is a better approximation than ignoring AA EV completely, but it can still result in substantial error. The SPD is more accurate still. For many choices of transfer parameters the latter does a good job of reproducing the simulations even when the CL method results in significant errors. However, for some choices of parameters and at high enough concentrations, all the analytical methods generate curves with significant error.

In Figure 4, the absolute results of the various calculations were presented. However, the most important aspect of the calculated $\langle P_{ct}(t)\rangle$ curves is not the absolute magnitude but rather the functional form. In an experiment, generally only the time-dependent shape of the curve can be measured; the absolute magnitude is subject to too many experimental uncertainties. As a result, the signal amplitude is obtained in arbitrary units and is scaled for comparison with theoretical calculations. In Figure 5 simulations are shown as calculated, but the analytical results have been scaled to match the simulations at the peak. The parameters are the same as in the previous figure. The agreement between the SPD method and simulation is seen to be quite good. For this concentration and selection of transfer parameters, the CL method is also close, while the calculation without AA EV is less accurate. For a wide range of concentrations and transfer parameters, the SPD approximation reproduces the simulated curves quite well. At lower concentrations the CL method is also quite good, but the error using it becomes substantial at concentrations or for ranges of transfer parameters for which the SPD method still works well. It is not possible to specify the exact concentration range over which the SPD method works well. The accuracy depends on the electron-transfer parameters and the concentration and on particle size. The number of acceptors is more important than the fractional occupancy of the space. For example, the SPD method works well for a 5% fractional occupancy if the acceptor radius is 5 Å even for electron-transfer parameters which give fast transfer, but it works poorly for the same fractional occupancy and electron-transfer parameters if the acceptor radius is 2.5 Å.

The SPD method works better for calculation of $\langle P_{ct}(t)\rangle$ than it does for $\langle P_{ex}(t)\rangle$. This is presumably due to a cancellation of errors, since $\langle P_{ex}(t)\rangle$ is an input into the calculation of $\langle P_{ct}(t)\rangle$. In addition, the $\langle P_{ex}(t)\rangle$ curves cannot be arbitrarily scaled, since the initial condition requires that they all begin at 1. Like the $\langle P_{ct}(t)\rangle$, the $\langle P_{ex}(t)\rangle$ curves match the simulations well for low-to-moderate concentrations, moderate-to-large size acceptors, and slow-to-moderate transfer parameters. Under the conditions of small particles (less than 3.5 Å radius), high concentrations ([C] > 0.4 M), and transfer parameters which give very fast transfer, the analytical methods, including the SPD method, can result in significant error. An example of this is seen in Figure 6 where the parameters were chosen (see figure caption) to generate a particularly unfavorable situation. As the figure

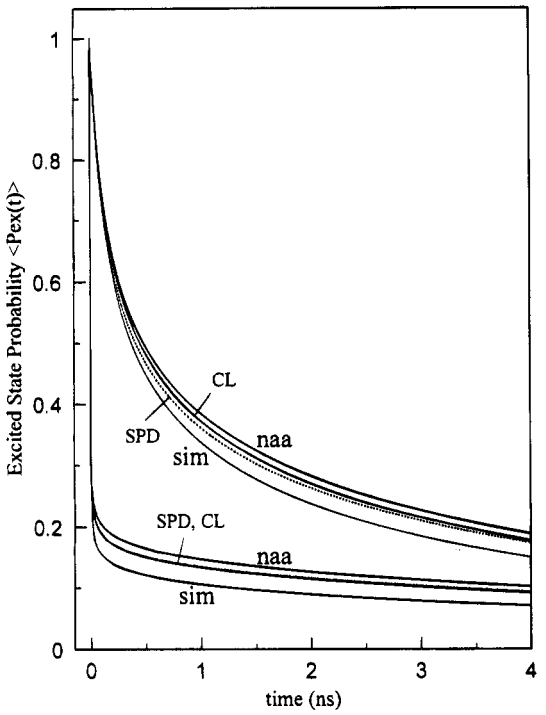

Figure 6. Excited state survival probability $\langle P_{ex}(t)\rangle$ for infinite 3D system with AA EV, calculated by several methods: MC simulations (sim), separable probability distribution (spd), continuum limit of the lattice model (CL), and exact theory with no inclusion of AA EV (naa). All molecules have a radius of 3.6 Å, calculated for an acceptor concentration of 0.445 M. Fluorescence lifetime $\tau = 15.0$ ns. The upper curves have forward electron transfer parameters $a_f = 0.9$, $R_f = 12.3$; the lower curves are $a_f = 0.22$, $R_f = 13.1$.

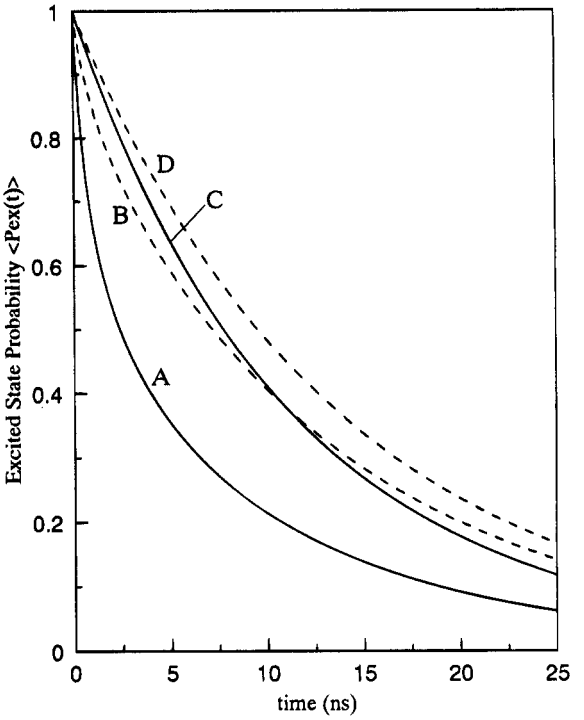

Figure 7. Comparison of excited state probability $\langle P_{ex}(t)\rangle$ simulation calculations for infinite 3D and micelle surface 2D systems for a fractional occupancy of 10%. All particles have a radius of 5.0 Å. Micelle radius $R_{mic} = 25.0$ Å. Excited-state lifetime $\tau = 15.0$. Solid curves A and C are simulations for the infinite 3D system, while the dashed curves B and D are the equivalent curves for the micelle. Curves A and B have electron transfer parameters of $a_f = 0.5$, $R_f = 12.0$. Curves C and D have parameters of $a_f = 1.0$, $R_f = 10.0$.

shows, the SPD and CL methods are an improvement over calculations that include only DA EV, but they still do not reproduce the simulations.

Similar comparisons were made for the micelle problem. There is no equivalent of the CL model, but calculations with DA EV only, the SPD method, and simulations with DA EV and AA EV were compared. Qualitatively the results are very similar. At concentrations for which AA EV is important, the SPD method always works better than ignoring AA EV. $\langle P_{ct}(t)\rangle$ curves are reproduced more accurately than $\langle P_{ex}(t)\rangle$ curves. At sufficiently high concentrations, deviations between the simulations and the SPD method become comparable to those shown in Figure 6. Examples of calculations for the micelle problem are presented elsewhere.[18]

vi. Comparison of Geometrical Effects on Electron-Transfer Rates. A comparison between the isotropic 3D and the micelle surface calculations can also be used to show the effects of restricted geometry on the dynamics of electron transfer. Figure 7 gives the excited-state probabilities, $\langle P_{ex}(t)\rangle$, for two sets of transfer parameters for both micelle and 3D geometries with both DA and AA EV, and Figure 8 gives the corresponding ion probabilities, $\langle P_{ct}(t)\rangle$. The calculations were obtained from the simulations with DA EV and AA EV. All the system variables were held constant between the two cases (see figure caption for parameters). For both systems, all particles had a radius of 5 Å. The number of particles in each system were chosen such that the fractional occupancy for each was equal to 10%. For these equal conditions, electron transfer in infinite 3D was found to be more rapid than for transfer on the surface of a micelle. This is true for any value of the transfer parameters or particle size, when equivalent values are used for the two systems. The reason for this difference in rates of transfer is the result of a competition of two factors: a change in the probability distribution of acceptors due to system topology, and a difference in absolute number of acceptors in each system, due in large part to the respective dimensionalities. The product of these two terms, $N \cdot P(R)$, gives the total number of particles at each distance r from the donor. For systems of low fractional occupancy (less than 5%), the probability distribution is known (AA EV is relatively unimportant in determining particle placement, and the probability distribution is equal to the $P(R)$ for the point particle acceptor case). This allows an a priori determination that, for equal fractional occupancies of particles, the number of acceptors at any distance from the donor is larger for the 3D case, and thus the rates of electron transfer will be greater. For larger fractional occupancies (>5%), computational comparisons find that this still is true.

IV. Concluding Remarks

It is possible to make some rough statements concerning the applicability of the various methods. Below a few percent occupancy in either an infinite 3D system or in a micelle system, AA EV does not make a significant difference in the calculation of observables. Below ~10% occupancy, the SPD method does a very reasonable job of reproducing the simulations. This is particularly true for $\langle P_{ct}(t)\rangle$ and therefore should provide a good approach to the interpretation of experimental results. However, given the discussions presented above, it is clear that no hard rules can be put down on ranges of applicability since the accuracy of a calculation, in regard to the influence of AA EV, depends on the interplay of a variety of parameters that define a particular electron-transfer system. Only a full simulation can test the accuracy of an analytical calculation when the parameters are of the type that can lead to error. However, given the vast reduction in computational time afforded by the analytical

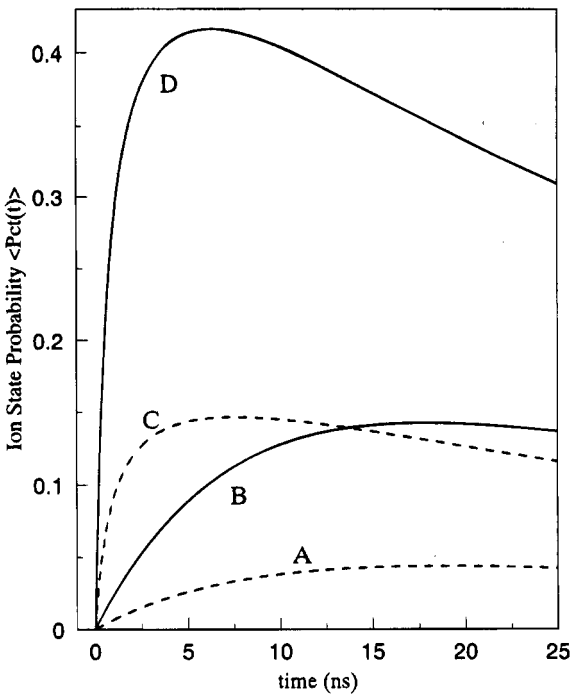

Figure 8. Comparison of ion state probability $\langle P_{ct}(t)\rangle$ simulation calculations for infinite 3D and micelle surface 2D systems. All particles have a radius of 5.0 Å. For 3D (solid curves B and D), acceptor concentration = 0.332 M. For micelle (dashed curves A and C), N = 10 particles and radius R_{mic} = 25.0 Å. Fluorescence lifetime τ = 15.0 ns. Electron-transfer parameters for curves A (micelle) and B (3D): $a_f = a_b = 1.0$, $R_f = R_b = 10.0$. Parameters for curves C (micelle) and D (3D): $a_f = 0.5$, $R_f = 12.0$, $a_b = 1.0$, $R_b = 10.0$.

theory, it is a useful approach to understanding photoinduced electron transfer with geminate recombination.

Future work will be focused on the effects of diffusion on photoinduced electron transfer and geminate recombination. The analytical method discussed above has been extended to include the influence of diffusion.[16,46] Once diffusion is included, it is possible for ions to separate and avoid geminate recombination. At high acceptor concentration, the CL model was previously employed to account for AA EV.[16,46] The analytical theory with diffusion is being extended to use the SPD method. In addition, MC simulations of the problem with diffusion are in progress. As in the study presented here, comparison between the analytical theory and the simulations will determine the accuracy of the analytical theory. The development of the theory for restricted geometries, exemplified by the micelle calculations, will permit experimental systems of this type to be studied quantitatively. Donor and acceptor molecules bound to the surface of a micelle is an experimentally realizable system. However, recent studies have shown that chromophores on micelle surfaces have significant surface diffusion constants.[47] Therefore the micelle theory will also be extended to include the influence of diffusion on forward transfer and geminate recombination. Micelles are only one example of a class of interesting restricted geometry electron-transfer systems. Considerable progress has been made on understanding the dynamics of excitation transfer for chromophores bound to polymer chains.[48,49] These studies have also been used as detailed probes of polymer structure and interactions. The restricted geometry theory of photoinduced electron transfer and geminate recombination will aid in understanding and designing such interesting electron-transfer systems.

The calculations presented in this paper provide a mathematical treatment of electron transfer described physically by a three-level system, and extensions of the model can be made to systems of any geometry. The ultimate purpose is to obtain expressions for the time-dependent physical observables and to make direct comparisons with experimental observations. However, an important extension of the above theory needs to be included before such comparisons can be made accurately. In addition to the solution structure introduced by donor and acceptor volumes, the effects of finite solvent volume and structure need to be included.[50-53] Rather than assuming the solvent to be a continuum, a more accurate description of the multiparticle structure must be used. This extension is important even when the acceptor density is low enough that they do not interact with each other, because interactions with solvent molecules can cause fluctuations in the donor–acceptor radial separation probability. Since electron transfer is typically a short-range process, these variations in local acceptor density can be a significant factor in particle distribution and overall transfer rates. As a result, it is not correct to assume a perfectly uniform distribution of particles. When the concentration of acceptors is low enough that AA EV is not important, the analytical theory can include this appropriate radial distribution function, and the ensemble average can still be performed exactly. When AA EV is important, approximate solutions, such as the SPD approach, can be readily modified to include the solvent perturbation. In the probability distribution $P'(R)$ used in the above calculations (eq 15), the pair correlation function $g(R)$ must include the solvent effects. By replacement of the two-particle $g(R)$ with a multiparticle correlation function obtained for a system containing donor, acceptor, and solvent molecules, the correct distribution can be obtained. Examples of multiparticle $g(R)$ can be obtained from the literature or directly from MC simulation (for example, see refs 36 and 38). Investigation of the effects of solvent molecules on the calculation of electron transfer probabilities by methods of simulation and analytical theories will be discussed in future work.

Acknowledgment. We would like to thank Professor H. C. Andersen for helpful suggestions about the MC simulations. Thanks also go the Stanford Center for Materials Research for providing partial support for the computer used in this work. This work was supported by the Department of Energy, Office of Basic Energy Sciences (Grant DE-FG03–84ER13251). K.W. was supported by a National Science Foundation predoctoral fellowship.

References and Notes

(1) Kestner, N. R.; Logan, J.; Jortner, J. *J. Phys. Chem.* **1974**, *78*, 2148.
(2) Jortner, J. *J. Chem. Phys.* **1976**, *64*, 4860.
(3) VanDuyne, R. P.; Fischer, S. F. *Chem. Phys.* **1974**, *5*, 183.
(4) Siders, P.; Marcus, R. A. *J. Am. Chem. Soc.* **1981**, *103*, 748.
(5) Warshel, A. *J. Phys. Chem.* **1982**, *86*, 2218.
(6) Huddleston, R. K.; Miller, J. R. *J. Phys. Chem.* **1982**, *86*, 200.
(7) Domingue, R. P.; Fayer, M. D. *J. Chem. Phys* **1985**, *83*, 2242.
(8) Siders, P.; Cave, R. J.; Marcus, R. A. *J. Chem. Phys.* **1984**, *81*, 5613.
(9) Strauch, S.; McLendon, G.; McGuire, M.; Guarr, T. *J. Phys. Chem.* **1983**, *87*, 3579.
(10) Rochester Symposium on Charge Transfer in Restricted Geometries. *J. Phys. Chem.* **1991**, *96*.
(11) Klafter, J.; Drake, J. M.; Levitz, P. *J. Lumin.* **1990**, *45*, 34.
(12) *Molecular Dynamics in Restricted Geometries*; Klafter, J., Drake, J. M., Eds.; John Wiley & Sons: New York, 1989.
(13) *Dynamical Processes in Condensed Molecular Systems*; Klafter, J., Jortner, J., Blumen, A., Eds.; World Scientific: Singapore, 1989.
(14) Inokuti, M.; Hirayama, F. *J. Chem. Phys.* **1965**, *43*, 1978.
(15) Lin, Y.; Dorfman, R. C.; Fayer, M. D. *J. Chem. Phys.* **1989**, *90*, 159.
(16) Fayer, M. D.; Song, L.; Swallen, S. F.; Dorfman, R. C.; Weidemaier, K. In *Ultrafast Dynamics of Chemical Systems*; Simon, J. D., Ed.; Kluwer Academic Publishers: Amsterdam, 1994; p 37.
(17) Dorfman, R. C. Thesis, Stanford University, 1992.

(18) Weidemaier, K.; Fayer, M.D. *J. Chem. Phys.*, in press.
(19) Tachiya, M. *J. Chem. Soc., Faraday Trans. 2* **1979**, *75*, 271.
(20) Tachiya, M.; Mozumder, A. *Chem. Phys. Lett.* **1974**, *28*, 87.
(21) Blumen, A.; Manz, J. *J. Chem. Phys.* **1979**, *71*, 4694.
(22) Blumen, A. *J. Chem. Phys.* **1980**, *72*, 2632.
(23) Baumann, J.; Fayer, M. D. *J. Chem. Phys.* **1986**, *85*, 4087.
(24) Dorfman, R. C.; Lin, Y.; Fayer, M. D. *J. Phys. Chem.* **1990**, *94*, 8007.
(25) Dorfman, R. C.; Tachiya, M.; Fayer, M. D. *Chem. Phys. Lett.* **1991**, *179*, 152.
(26) Lin, Y.; Dorfman, R. C.; Fayer, M. D. *J. Chem. Phys.* **1990**, *93*, 3550.
(27) Marsaglia, G.; Zaman, A. *J. Appl. Prob.* **1991**, *1*, 1.
(28) James, F. *Comput. Phys. Comm.* **1990**, *60*, 329.
(29) Finger, K. U.; Marcus, A. H.; Fayer, M. D. *J. Chem. Phys.* **1994**, *100*, 271.
(30) Tobochnik, J.; Chapin, P. M. *J. Chem. Phys.* **1988**, *88*, 5824.
(31) Press, W. H.; Flannery, B. P.; Teukolsky, S. A.; Vetterling, W. T. *Numerical Recipes in C*; Cambridge University Press: Cambridge, 1988.
(32) Peterson, K. A.; Fayer, M. D. *J. Chem. Phys.* **1986**, *85*, 4702.
(33) Ediger, M. D.; Domingue, R. P.; Fayer, M. D. *J. Chem. Phys.* **1984**, *80*, 1246.
(34) Marcus, A. H.; Fayer, M. D.; Curro, J. G. *J. Chem. Phys.* **1994**, *100*, 9156.
(35) Kranendonk, W. G. T.; Frenkel, D. *Mol. Phys.* **1988**, *64*, 403.
(36) Hansen, J. P.; McDonald, I. R. *Theory of Simple Liquids*; Academic Press, Inc.: London, 1976.
(37) Allen, M. P.; Tildesley, D. J. *Computer Simulation of Liquids*; Clarendon Press: Oxford, 1987.
(38) Perram, J. W. *Mol. Phys.* **1975**, *30*, 1505.
(39) Wertheim, M. S. *J. Math. Phys.* **1964**, *5*, 643.
(40) Thiele, E. *J. Chem. Phys.* **1963**, *39*, 474.
(41) Glandt, E. D.; Kofke, D. A. *Mol. Phys.* **1988**, *64*, 125.
(42) Smith, W. R.; Henderson, D. *Mol. Phys.* **1970**, *19*, 411.
(43) Throop, G. J.; Bearman, R. J. *J. Chem. Phys.* **1964**, *42*, 2408.
(44) Haile, J. M. *Molecular Dynamics Simulation*; John Wiley & Sons: New York, 1992.
(45) Valleau, J. P.; Whittington, S. G. In *Statistical Mechanics*; Berne, B. J., Ed.; Plenum Press: New York, 1977; Vol. 5.
(46) Song, L.; Swallen, S. F.; Dorfman, R. C.; Weidemaier, K.; Fayer, M. D. *J. Phys. Chem.* **1993**, *97*, 1374.
(47) Quitevis, E. L.; Marcus, A. H.; Fayer, M. D. *J. Phys. Chem.* **1993**, *97*, 5762.
(48) Peterson, K. A.; Stein, A. D.; Fayer, M. D. *Macromolecules* **1990**, *23*, 111.
(49) Marcus, A. H.; Diachun, N. A.; Fayer, M. D. *Macromolecules* **1993**, *26*, 3041.
(50) Rice, S. A. *Diffusion-Limited Reactions*; Elsevier: Amsterdam, 1985.
(51) Northrup, S. H.; Hynes, J. T. *Chem. Phys. Lett* **1977**, *54*, 244.
(52) Northrup, S. H.; Hynes, J. T. *J. Chem. Phys.* **1979**, *71*, 871.
(53) Emeis, C. A.; Fehder, P. L. *J. Am. Chem. Soc.* **1970**, *92*, 2246.

JP942301Z